Journal of Electromyography and Kinesiology 47 (2019) 105–112

Contents lists available at ScienceDirect

Journal of Electromyography and Kinesiology

journal homepage: www.elsevier.com/locate/jelekin

Use of accelerometers for automatic regional chest movement recognition during tidal breathing in healthy subjects

Carlos De la Fuente[a,b,c,e], Alejandro Weinstein[d,e], Rodrigo Guzman-Venegas[a], Juan Arenas[b], Jorge Cartes[b], Marcos Soto[b], Felipe P. Carpes[f,*]

[a] Laboratorio integrativo de biomecánica y fisiología del esfuerzo, LIBFE, Escuela de Kinesiología, Universidad de los Andes, Santiago, Chile
[b] Carrera de Kinesiología, Departamento de Ciencias de la Salud, Facultad de Medicina, Pontificia Universidad Católica, Santiago, Chile
[c] Centro de Salud Deportivo, Clínica Santa María, Santiago, Chile
[d] School of Biomedical Engineer, Universidad de Valparaiso, Valparaíso, Chile
[e] Magíster en Ciencias de la Ingenieria, School of Biomedical Engineer, Universidad de Valparaiso, Valparaíso, Chile
[f] Applied Neuromechanics Research Group, Universidade Federal do Pampa, Campus Uruguaiana, Uruguaiana, Brazil

ARTICLE INFO

Keywords:
Chest wall
Abdominal wall
Machine learning
Clustering
Wearable technology

ABSTRACT

Recognition of breathing patterns helps clinicians to understand acute and chronic adaptations during exercise and pathological conditions. Wearable technologies combined with a proper data analysis provide a low cost option to monitor chest and abdominal wall movements. Here we set out to determine the feasibility of using accelerometry and machine learning to detect chest-abdominal wall movement patterns during tidal breathing. Furthermore, we determined the accelerometer positions included in the clusters, considering principal component domains. Eleven healthy participants (age: 21 ± 0.2 y, BMI: 23.4 ± 0.7 kg/m^2, FEV_1: 4.1 ± 0.3 L, VO_2: 4.6 ± 0.2 mL/min kg) were included in this cross-sectional study. Spirometry and ergospirometry assessments were performed with participants seated with 13 accelerometers placed over the thorax. Data collection lasted 10 min. Following signal pre-processing, principal components and clustering analyses were performed. The Euclidean distances in respect to centroids were compared between the clusters ($p < 0.05$), identifying two clusters ($p < 0.001$). The first cluster included sensors located at the right and left second rib midline, body of sternum, left fourth rib midline, right and left second thoracic vertebra midline, and fifth thoracic vertebra. The second cluster included sensors at the fourth right rib midline, right and left seventh ribs, abdomen at linea alba, and right and left tenth thoracic vertebra midline. Costal-superior and costal-abdominal patterns were also recognized. We conclude that accelerometers placed on the chest and abdominal wall permit the identification of two clusters of movements regarding respiration biomechanics.

1. Introduction

Three patterns have been described for chest-abdominal wall movements during breathing: costal-superior, costal-abdominal, and mixed; the costal-abdominal pattern is more common among healthy individuals (Ratnovosky et al., 2008, Bianchi et al., 2007; Stendardi et al., 2007; Massaroni et al., 2017). Despite this, different patterns still are observed among individuals without pathology, e.g., unlike the pattern in men, women usually show a costal-superior pattern during deep breathing (Ragnarsdóttir and Kristinsdóttir, 2006). The recognition of chest and abdominal wall movements is important because in many cases these patterns can be related to specific characteristics of populations and dysfunctions, like the costal-superior and costal-abdominal patterns in bronchial obstruction syndrome and quiet breathing, respectively (Bianchi et al., 2007; Takashima et al., 2017).

Changes in chest and abdominal wall movements aim to maintain a stable tidal volume through the modification of the breathing rate (Ratnovosky et al., 2008; Sarkar et al., 2015). These modifications increase recruitment of respiratory muscles to create a pressure gradient by upward and downward movements of the rib cage and/or posture (Takashima et al., 2017; Mesquita Montes et al., 2017) in combination with the activity of inspiratory and expiratory muscles (Ratnovosky et al., 2008; Maarsingh et al., 2000). The recognition of pattern through movement analysis might help to monitor changes in cardiorespiratory responses during rehabilitation, for example, in cases of dyspnea during respiratory exercises (Stendardi et al., 2007; Ziegler et al., 2015).

* Corresponding author.
E-mail addresses: delafuentte@gmail.com (C. De la Fuente), alejandro.weinstein@uv.cl (A. Weinstein), rguzman@uandes.cl (R. Guzman-Venegas), aarenaso@uc.cl (J. Arenas), jncartes@uc.cl (J. Cartes), masoto9@uc.cl (M. Soto), carpes@unipampa.edu.br (F.P. Carpes).

https://doi.org/10.1016/j.jelekin.2019.05.016
Received 27 August 2018; Received in revised form 11 May 2019; Accepted 23 May 2019

Identifying patterns of chest and abdominal wall movements using traditional methods like optoelectronic plethysmography (Aliverti et al., 2009; Takashima et al., 2017) and tridimensional photogrammetry (Takashima et al., 2017; Massaroni et al., 2017; De Groote et al., 1997) is difficult in the context of rehabilitation and clinical practice, mainly due to the environmental conditions and limitations in providing quick data collection and analysis. Therefore, pattern recognition tools that permit quick data collection and analysis are of interest to clinicians. In this regard, wearable non-invasive technologies such as accelerometers are useful (Kavanagh and Menz, 2008). Accelerometers placed on the abdominal wall were successfully used to monitor the diaphragmatic activity while under anesthesia (Drummond et al., 2013), and wearable accelerometers placed on the abdominal wall and rib cage helped to identify normal, bradypnea, tachypnea, kussmaul, apneustic, Biot's respiration, sighing and Cheyne-Stokes patterns (Fekr et al., 2016). This suggests that breathing movements can be quantified and monitored through accelerometers, which may provide a good framework for identifying patterns of movements. Despite of this, the use of accelerometry to quantify chest movements that can help to describe respiratory movements and postures still lacks in the literature. Specific postures are known to influence patterns of chest and abdominal wall movements (Reifferscheid et al., 2011; Takashima et al., 2017). For example, the seated position favors a better action of diaphragm in increasing the transverse diameter of the lower rib cage (costal-diaphragmatic pattern). The excursion of diaphragm is more related with the descending of its central tendon and consequently with the abdominal wall movement (Takazakura et al., 2004).

Most of previous studies addressed the quantification of different patterns of chest and abdominal wall movements without considering anatomical references. In previous studies, one, two or multiples accelerometers were placed arbitrarily on sites of the chest and abdominal wall to perform the recognition (Drummond et al., 2013; Fukakusa et al., 1998; Fekr et al., 2016; Liu et al., 2017). We considered that placing the sensors on sites based on anatomical references from the chest and abdominal wall could provide relevant information regarding the costal-superior or costal-abdominal regions. In this regard, specific sites related to clinical practice would also be useful in facilitating the placement of sensors when assessing different individuals. How to process this information is also a matter of discussion. Cluster analysis permits the assignment of variables to specific homogeneous groups that were different from other groups and may also permit the discovery of patterns behind the data. K-means is a popular cluster algorithm to perform the partition of n observations into k clusters that are representative of the objects associated with the cluster. However, results from large or high dimensional datasets may not be accurate if the dimension is not reduced previously, which can be performed by applying a principal component analysis technique that reduces the number of dimensions without significant loss of information (Prabhu and Anbazhagan, 2011). Such data processing approaches can be useful to determine regional patterns of motion from the chest and abdominal wall.

There is a lack of evidence regarding the use of accelerometry signals from sensors placed on the thorax and abdominal wall to recognize chest-abdominal wall patterns during breathing exercises in a typical clinical posture (i.e., seated position) as suggested by Price et al. (2014). Here we set out to determine the feasibility of using accelerometry and machine learning algorithms to detect chest-abdominal wall patterns during tidal breathing. The memberships of sensors in the principal component domain between the identified clusters were also determined. We hypothesized that two respiratory patterns could be recognized using principal components in combination with k-means.

Table 1
Characteristics of the participants included in the study.

Demographic characteristics	Mean (standard deviation)
Sex, male/female	6/5
Age, years	21.0 (0.2)
Height, m	1.70 (0.21)
Weight, kg	67.9 (3.2)
BMI, kg/m^2	23.4 (0.7)
Spirometry characteristics	
FEV_1, L	4.06 (0.29)
FEV_1, %	94.0 (3.6)
FVC, L	4.77 (0.34)
FVC, %	93.6 (2.9)
FEV_1/FCV, L/L	85.3 (2.1)
FEF_{25-75}, L/s	4.32 (0.43)
FEF_{25-75}, %	91.0 (7.1)
Ergospirometry characteristics	
breathing rate, rpm	11.6 (1.4)
VC, L	0.81 (0.10)
VE, L/min	8.63 (0.47)
relative VO_2, mL/min/Kg	4.63 (0.15)
absolute VO_2, mL/min	314.55 (20.32)
VCO_2, mL/min	240.66 (15.12)

BMI = body mass index. FEV_1 = forced expiration volume at the end of first second. FVC = forced vital capacity. FEF_{25-75} = forced expiratory flow between 25 and 75 percent. VC = vital capacity. VE = exhaled volume. VO_2 = relative volume of consumption. absolute VO_2 = absolute volume of consumption. VCO_2 = carbon dioxide consumption.

2. Methods

2.1. Study design

This cross-sectional observational analytic study was approved by the IRB from Pontificia Universidad Católica de Chile and conducted according to the Helsinki declaration.

2.2. Participants

To explore the feasibility of using accelerometers to recognize breathing patterns without the influence of pathology, eleven healthy participants (5 women and 6 men) were included in this research. Table 1 summarizes the characteristics of the participants. The inclusion criteria were: (i) age between 18 and 25 years old, (ii) physically active profile (more than 150 min of physical activity per week) and (iii) normal lung function assessed by spirometry values. The exclusion criteria were: (i) smoking, (ii) thoracic structure abnormality, (iii) presence of pain, (iv) infection episode within the last month, (v) elite or recreational sport practice (specific performance training during the last 6 months), (vi) presence of allergic signs and symptoms, (vii) bronchodilator use or dependence, (viii) recent pharmacological treatment and (ix) chronic cardiorespiratory disease.

2.3. Instruments

A portable spirometer ML3500 model (Carefusion, Inc., San Diego, USA), a Carefusion ergoespirometer (JägerTM, Würzburg, German), and a Trigno™ accelerometry system (Delsys inc., USA) were employed for data collection. The accelerometers sensors had 3 degrees of freedom, range of ± 3 g, sampling resolution of 20 ± 5 Hz, > 40 dB*dec^{-1} and 450 ± 50 Hz > 80 dB*dec^{-1}, basal

noise (rms) of 0.016 g for range ± 1.5 g and 0.032 g for range ± 6 g, bandwidth of DC − 50 ± 5 Hz with 20 dB*dec^{-1}, offset error of ± 0.21 g for XY axis and −0.42 g for Z axis, and accelerometer resolution depth of 10 bits.

2.4. Procedures

Before accelerometry data collection, a senior health professional performed all spirometry assessments using the portable spirometer according to the criteria established by the American Thoracic Society and the European Respiratory Society (Miller et al., 2005). Results were interpreted according to the reference values from Knudson et al. (1983). At the start of the analysis, each participant adopted a relaxed seated posture and performed tidal respirations for 10 min. The participants were assessed using a disposable paperboard spirometry nozzle on the mouth, with nose clamped and a disposable filter in the spirometry. Then, the participants performed five tidal ventilations before a maximal inhalation with pauses of 2 s to expire all air that they could (Gutierrez et al., 2007). The three best attempts were recorded for each participant.

After spirometry assessment, participants were seated with hip, knee and ankle at 90° of flexion, trunk vertically aligned to the gravity vector and arms resting along the thigh. As described by Price et al. (2014), this posture was assumed to improve the postural stability during the test and to better control the weight and height of connection with the ergospirometer. Participants were connected to the ergoespirometer through a mouth-adapter and using a nasal clip (JägerTM, Würzburg, German), and visual feedback of their respiration (oxygen uptake flow) was provided while maintaining a normal tidal volume for 10 min. Data were collected at 0.2 Hz through J-Lab software (Jäger™, Würzburg, German) and samples of VO_2 data were recorded each second in tidal breathing (~12 breaths per minute) as recommended by Robergs et al. (2010). During the spirometry assessment, 13 wireless accelerometers sampled data at 148.15 Hz (Delsys, Inc., Boston, USA). The accelerometers were attached to the participant thorax and abdominal skin over 10 auscultations points and 3 non-auscultation points from the anterior front plane of thorax: (i) midline from right and left second rib, (ii) body of sternum, (iii) midline from right and left fourth ribs, (iv) right and left seventh ribs and (v) at the abdominal level at linea alba. Five sensors were placed on the posterior front plane of the thorax at (i) midline from right and left second thoracic vertebra, (ii) fifth thoracic vertebra and (iii) midline from right and left tenth thoracic vertebra. The selection of these sites permitted the use of familiar clinical landmarks known by respiratory clinicians and tracked different zones of the thorax and the abdominal wall, also ensuring a symmetrical distribution of accelerometers. A fourteenth sensor was placed on a table and remained at rest to serve as a control, as Fig. 1 illustrates. All accelerometer data were collected using EMG works 4.1.1. (Delsys, Boston, USA) and analyzed using custom-made scripts written in Matlab 2016a software (Mathworks Inc., Massachusetts, USA).

2.5. Variables and data processing

The magnitude of acceleration, which was determined from accelerometer data, was defined by the Euclidean distance of three orthogonal vectors that were periodically acquired by the tri-axial accelerometers that performed measurements at 13 anatomical positions distributed on the chest, thorax and abdominal wall. It was a continuous variable expressed relative to the gravity acceleration (g). As part of the pre-processing procedures, the magnitudes of acceleration were obtained to reduce the tri-axial accelerometer data. One thousand central samples were extracted to pre-process and analyze, and a smooth method was performed using a simple moving average of 100 samples, with passes occurring sample-to-sample to improve the peak-to-peak breath of the accelerometry signals. Then, a second-order, zero lag, low-pass Butterworth filter with a cut-off frequency of 0.5 Hz was applied to attenuate artifacts that were not smoothed by the mean average. Finally, the data were standardized by z-scores. All procedures were conducted using Matlab 2016a software (Mathworks Inc., Massachusetts, USA).

A principal component analysis (PCA) was performed in the time domain, using the covariance matrix to reduce the dimensionality of the dataset. This method maximized the variance of data by orthogonal transformation. The covariance matrix was used to obtain a square matrix $\Re^{1000x1000}$. Then, an eigendecomposition, satisfying Eq. (1) (where λ is the eigenvalues matrix, v the eigenvector matrix and A the obtained covariance matrix), was solved by finding multiple eigenvalue equations (Eq. (2), where I is the identity matrix). Then, the principal component matrix was created by multiplying the original raw matrix

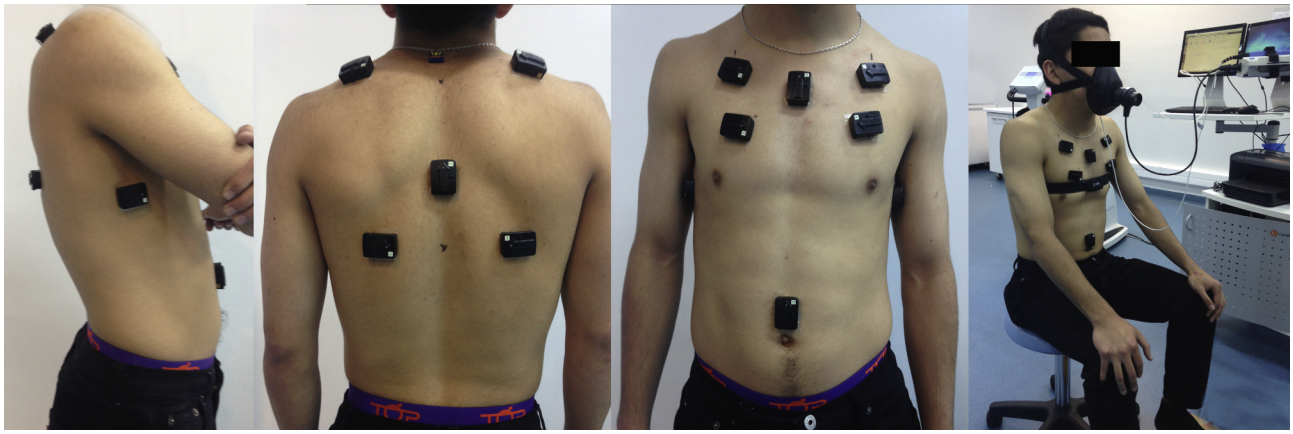

Fig. 1. Setup of accelerometer positioning. Ergospirometer mask and accelerometry sensors were placed on specific body sites of the participants. The accelerometers were placed on the anterior frontal plane of the thorax at: (i) the midline from the right and left second rib, (ii) the body of the sternum, (iii) the midline from right and left fourth rib, (iv) midline from right and left seventh rib, and (v) at the abdominal level at linea alba. Five sensors were placed in the posterior frontal plane of the thorax at: (i) the midline from right and left second thoracic vertebra, (ii) the fifth thoracic vertebra, and (iii) the midline from the right and left tenth thoracic vertebra. A fourteenth sensor stayed at rest on a table to serve as a control sensor.

Table 2
Mean, RMS and variance of segmented acceleration by participants.

		Normalized acceleration respect to the reference sensor no.14 (at rest on a table)												
		1	2	3	4	5	6	7	8	9	10	11	12	13
#1	Mean	1.7589	2.1902	1.8331	1.6984	1.8583	1.7560	1.5605	1.7407	1.5484	1.4534	1.5289	1.7361	1.6286
	RMS	1.7589	2.1903	1.8331	1.6984	1.8584	1.7560	1.5605	1.7407	1.5484	1.4534	1.5290	1.7362	1.6286
	Variance*10^{-3}	0.0023	0.1562	0.0252	0.0292	0.4508	0.0217	0.0048	0.0203	0.0007	0.0008	0.0159	0.0458	0.0169
#2	Mean	1.4583	1.7992	1.5035	1.4004	1.5898	1.3832	1.2409	1.3457	1.3394	1.2229	1.2931	1.1742	1.1433
	RMS	1.4583	1.7993	1.5036	1.4004	1.5899	1.3832	1.2409	1.3457	1.3394	1.2229	1.2931	1.1742	1.1433
	Variance*10^{-3}	0.0007	0.1491	0.0600	0.0626	0.4543	0.0074	0.0007	0.0056	0.0027	0.0048	0.0131	0.0242	0.0019
#3	Mean	1.6107	2.0576	1.6437	1.5416	1.6654	1.6274	1.3760	1.5076	1.4571	1.4388	1.5024	1.5903	1.4337
	RMS	1.6107	2.0576	1.6437	1.5416	1.6654	1.6274	1.3760	1.5077	1.4571	1.4388	1.5024	1.5903	1.4337
	Variance*10^{-3}	0.0013	0.0437	0.0298	0.0072	0.1110	0.0009	0.0078	0.0246	0.0009	0.0100	0.0134	0.0078	0.0021
#4	Mean	1.9251	2.3528	1.9908	1.8862	2.1576	1.8791	1.7178	1.9342	1.7431	1.5923	1.6604	1.7951	1.6051
	RMS	1.9251	2.3528	1.9908	1.8862	2.1576	1.8791	1.7178	1.9342	1.7431	1.5923	1.6605	1.7951	1.6051
	Variance*10^{-3}	0.0008	0.0297	0.0159	0.0057	0.1466	0.0275	0.0166	0.0825	0.0042	0.0247	0.0157	0.0173	0.0112
#5	Mean	1.5546	1.9677	1.5811	1.4635	1.5170	1.5221	1.3784	1.5501	1.3697	1.3048	1.3208	1.5073	1.3113
	RMS	1.5546	1.9677	1.5811	1.4635	0.5170	1.5221	1.3784	1.5501	1.3697	1.3048	1.3208	1.5073	1.3113
	Variance*10^{-3}	0.0094	0.4541	0.1539	0.0456	0.2273	0.0080	0.0505	0.0706	0.0859	0.0192	0.3622	0.1881	0.0426
#6	Mean	1.6637	2.0306	1.7136	1.6365	1.9212	1.5305	1.3406	1.4161	1.4542	1.3574	1.3624	1.7191	1.4603
	RMS	1.6637	2.0306	1.7136	1.6365	1.9212	1.5305	1.3406	1.4161	1.4542	1.3574	1.3624	1.7191	1.4603
	Variance*10^{-3}	0.0022	0.0552	0.0195	0.0184	0.0510	0.1283	0.0414	0.0145	0.0164	0.0047	0.0440	0.0345	0.1547
#7	Mean	1.5221	1.9042	1.5264	1.3990	1.4262	1.5121	1.3546	1.4542	1.2530	1.2490	1.3077	1.4708	1.3920
	RMS	1.5222	1.9043	1.5264	1.3990	1.4262	1.5121	1.3546	1.4542	1.2530	1.2490	1.3077	1.4708	1.3920
	Variance*10^{-3}	0.4617	0.3549	0.0104	0.0076	0.0300	0.0018	0.0019	0.0139	0.0066	0.0084	0.0056	0.0071	0.0029
#8	Mean	1.8497	2.2067	1.9278	1.7781	2.0035	1.7684	1.6078	1.7982	1.5923	1.5249	1.5073	1.9148	1.6436
	RMS	1.8497	2.2068	1.9278	1.7781	2.0037	1.7684	1.6078	1.7982	1.5923	1.5249	1.5073	1.9148	1.6437
	Variance*10^{-3}	0.0019	0.1562	0.0279	0.0779	0.8479	0.0031	0.0132	0.0837	0.0109	0.0014	0.0670	0.0567	0.2042
#9	Mean	1.5808	1.8986	1.6494	1.5452	1.7804	1.5029	1.3256	1.4231	1.3826	1.3103	1.3449	1.5621	1.3704
	RMS	1.5808	1.8987	1.6494	1.5452	1.7805	1.5029	1.3256	1.4232	1.3826	1.3103	1.3449	1.5621	1.3704
	Variance*10^{-3}	0.0679	0.0380	0.0049	0.0085	0.1335	0.0102	0.0292	0.0760	0.0046	0.0056	0.0085	0.0240	0.0025
#10	Mean	1.9560	2.4689	1.9677	1.8750	2.1093	1.8867	1.6328	1.7754	1.7484	1.6598	1.7617	1.8687	1.7830
	RMS	1.9560	2.4689	1.9677	1.8750	2.1093	1.8867	1.6328	1.7754	1.7484	1.6598	1.7617	1.8687	1.7830
	Variance*10^{-3}	0.0395	0.1031	0.0309	0.0096	0.0753	0.0221	0.0038	0.0057	0.0016	0.0029	0.0021	0.0011	0.0207
#11	Mean	1.9258	2.4870	1.8997	1.8110	2.0085	1.8355	1.5092	1.5630	1.6038	1.5120	1.7974	1.6760	1.5794
	RMS	1.9259	2.4870	1.8997	1.8114	2.0085	1.8355	1.5092	1.5630	1.6038	1.5125	1.7974	1.6761	1.5795
	Variance*10^{-3}	0.0004	0.0001	0.0000	0.0014	0.0001	0.0000	0.0000	0.0000	0.0000	0.0013	0.0000	0.0002	0.0004

with the three most weighting eigenvectors, diminishing the original dimensionality of $\Re^{1000x143}$ to $\Re^{3x143}$, thus improving the computational cost and accuracy (Prabhu and Anbazhagan, 2011). The criteria to determine the number of the eigenvalues used included the nearest value greater than or equal to 0.90 of cross-correlation coefficient between the non-standardized and reconstructed signal. The variance of each component also was determined. All procedures were conducted using Matlab 2016a software (Mathworks Inc., Massachusetts, USA).

$$Av = \lambda v \tag{1}$$

$$(A - \lambda_i I)v = 0 \tag{2}$$

To determine what accelerometry information was related to the patterns of chest-abdominal wall, a machine learning K-means clustering algorithm was performed in the principal components domain. The algorithm grouped data into smaller groups by Euclidean distance similarities. The algorithm partitions n samples ($x_i = 1,\ldots, n$ with j dimensions corresponding to the number of principal components) into k clusters in a random manner to find the position μ of the cluster, minimizing the square Euclidean distance d' from the samples within each cluster until convergence, as Eq. (3) summarizes. All procedures were conducted in Matlab 2016a software (Mathworks Inc., Massachusetts, USA).

$$\min_{c} \sum_{i=1}^{k} \sum_{x \in c_i} d'(x^j, \mu_i) = \min_{c} \sum_{i=1}^{k} \sum_{x \in c_i} ||x^j - \mu_i||_2^2 \tag{3}$$

To assess whether the features of mean, root mean square and variance of normalized magnitude of accelerations (comparing all sensors using one-way ANOVA and multiple comparison with $p < 0.05$) result in similar recognition, the outcomes of PCA with dimension reduction were compared to outcomes from K-means. As shown in Fig. 3, K-means from the magnitude of accelerations give outcomes similar to PCA with dimension reduction.

2.6. Statistical analysis

Data are reported as mean and standard deviation. The Shapiro-Wilk test confirmed the normality of data distribution. Homoscedasticity was confirmed using Levene's test. To determine which of the sensors belonged to each cluster, cluster one and two recognized in the PCA domain were compared. Statistical significance

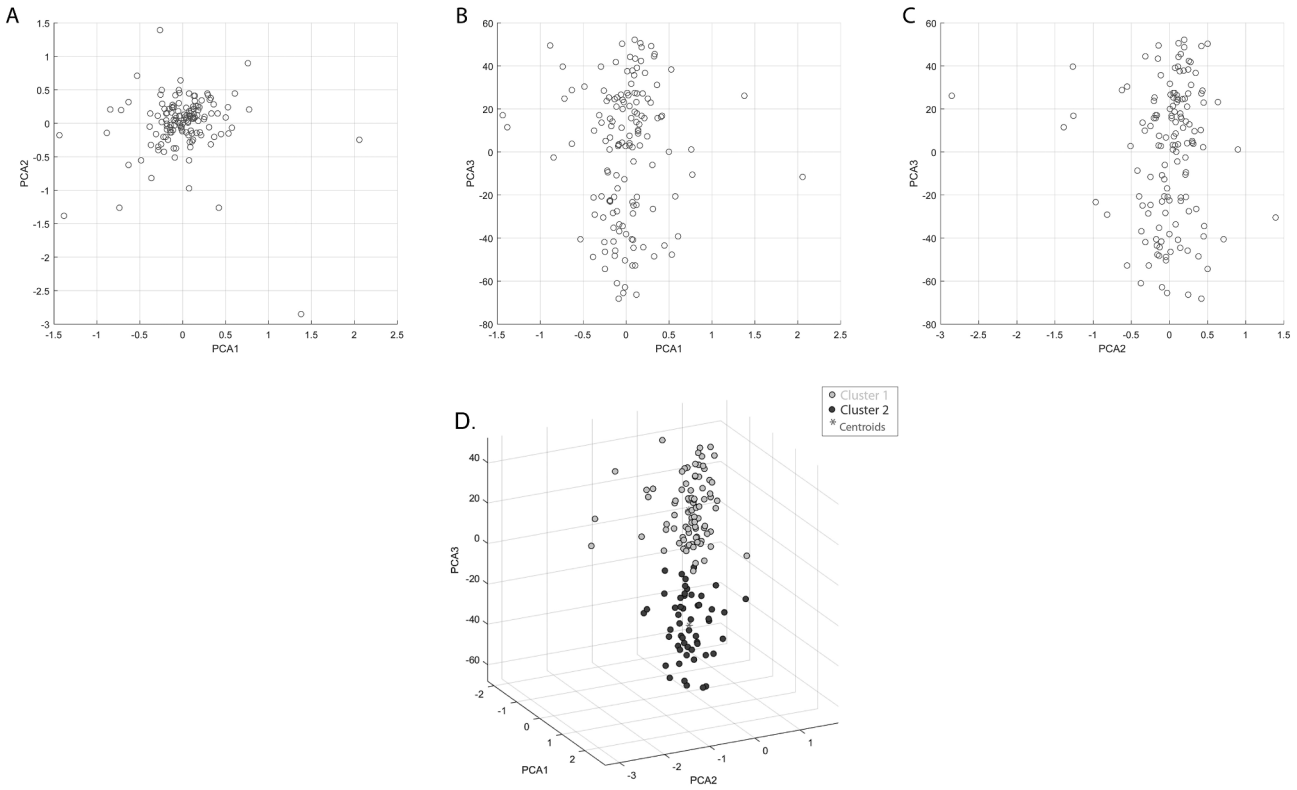

Fig. 2. Principal component analysis. The image shows each accelerometer in the principal component domain. (A) Weight coefficient of first vs. second principal components. (B) Weight coefficient of first vs. third principal components. (C) Weight coefficient of second vs. third principal components. (D) Tridimensional organization of two clusters with their centroids in the principal component domain: the first cluster is in light gray, the second cluster in dark gray, and the centroids of clusters are in asterisk.

Table 3
Cluster proportion of PCA with dimension reduction and K-means.

	Cluster one	Cluster two	z-score	p-value
Anterior frontal plane				
2nd right rib	11/11	0/11	−4.6904	< 0.0001
2nd left rib	11/11	0/11	−4.6904	< 0.0001
4th right rib	0/11	11/11	−4.6904	< 0.0001
4th left rib	11/11	0/11	−4.6904	< 0.0001
body of sternum	11/11	0/11	−4.6904	< 0.0001
7th right rib	0/11	11/11	−4.6904	< 0.0001
7th left rib	0/11	11/11	−4.6904	< 0.0001
abdominal at alba's line	1/11	10/11	−3.8376	0.0001
Posterior frontal plane				
2nd right thoracic vertebra	11/11	0/11	−4.6904	< 0.0001
2nd left thoracic vertebra	11/11	0/11	−4.6904	< 0.0001
5th thoracic vertebra	11/11	0/11	−4.6904	< 0.0001
10th right rib	11/11	0/11	−4.6904	< 0.0001
10th left rib	3/11	8/11	−2.1320	0.0332

Data are presented as proportions (identified case/sample). The control sensor remained at rest and was always identified as part of cluster one.

($p < 0.05$) was determined by performing a two-tailed test for two population proportions. The null-hypothesis assessed was p_1-$p_2 = 0$, where p was the proportions values. The numbers of cluster were determined using the major silhouette coefficient, which assessed 1 to 10 clusters. The analyses were performed using the statistical toolbox from Matlab 2016a software (Mathworks Inc., Massachusetts, USA). The statistical power of the study was estimated by *post-hoc* analysis, considering the larger proportion obtained, using G*Power 3.1.9.2 (Universität Kiel, Germany).

3. Results

Table 2 summarizes the mean, root mean square (RMS) and variance obtained for each participant, and Fig. 2 shows the PCA outcomes. The total variance explained by the first, second and third principal component were 31.09%, 25.16% and 19.14%, respectively, which explained 75.39% of the total variance. Three were chosen for the eigenvalues due to the cross-correlation coefficient (r = 0.91) found between the non-standardized and reconstructed signals from PCA. The silhouette coefficient for two clusters showed the highest cross-correlation coefficient (r = 0.89). Therefore, two clusters in the domain of principal components were identified (see Table 2 and Fig. 3). Sensor location in a particular cluster is summarized in Table 3. The first cluster brought together sensors located at midline of the right and left second rib, the body of the sternum, midline of the left fourth rib, midline of the right and left second thoracic vertebra, and the fifth thoracic vertebra. The second cluster brought together sensors located at midline from right fourth rib, right and left seventh ribs, the abdomen at linea alba, and the right and midline from the left tenth thoracic vertebra. Therefore, two clusters organized anatomically were identified using principal components analysis and the K-means algorithm. A *post-hoc* analysis showed a statistical power of 0.996 when the proportion of tenth left rib was assessed, which was the highest proportion found.

Fig. 3 summarizes results of sensor distribution using the mean, RMS, variance and K-means on the magnitude of accelerations, non-dimension reduction with PCA and K-means, and PCA with dimension reduction.

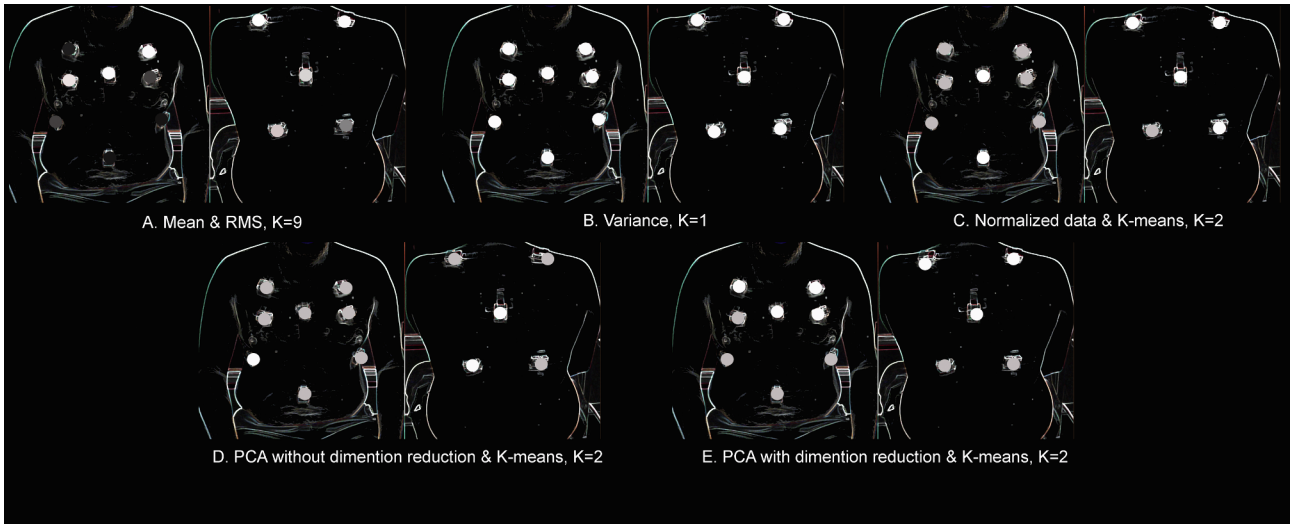

Fig. 3. Tidal breathing pattern recognition. Clusters are showed in gray scale, representing: (A) multiple comparisons of mean and RMS ($p < 0.001$) found 9 groups; (B) multiple comparisons of variance ($p = 0.088$) found one group; (C) K-means applied for normalized data using two clusters; (D) K-means applied for principal component domain without dimension reduction; (E) K-means applied on principal component domain with dimension reduction using three principal components.

4. Discussion

The main finding of our study is that accelerometers placed on skin over the abdominal wall and thorax in healthy participants permits the identification of two accelerometry patterns during tidal breathing in the seated posture. The accelerometry patterns and the machine learning algorithm employed here suggest that costal-superior and costal-abdominal patterns can be detected by accelerometers localized on upper and lower chest and abdominal wall.

The placement of the accelerometers seemed to be crucial to the outcomes. Specific sites related to the clinical practice of auscultation were selected to make it easier for clinicians when preparing the participant for assessment. We also included a few other sites that can be easily placed with the consideration of some anatomical references. Sensors placed on the thorax and abdominal wall permitted the recognition of two patterns based on the similitude of the Euclidean distance found in the principal component domain, in which the data were separated into two clusters. Our approach differs from methods using one, two or more accelerometers to classify a breath pattern associated with a pathology (Fekr et al., 2016) because we consider that our findings are more representative of the breathing movements, and our approach permits the identification of these movements without the need to use multiple reflective markers on chest and abdominal wall, like the approach performed using kinematics described in Takashima et al. (2017).

The two patterns recognized suggest the existence of regional differences for tidal breath in the seated position. This is in accordance with the different thoracic and abdominal wall movements, where the thorax and abdominal diameters change more in the caudal than the cranial direction (Takashima et al., 2017). This is also in agreement with the lung weight leading to a regional effect on ventilation in a seated position, which reflects the different distribution of inspired air between the superior and inferior lung layers (Reifferscheid et al., 2011). As the underlying lung tissue is distant from the diaphragm and rib cage movement, and the changes in the cross-sectional area differ between the cranial and caudal chest (Reifferscheid et al., 2011), our method recognizes two different patterns of ventilation using non-supervised data analysis that includes principal component analysis after K-means clustering. The physiological meaning of our findings concerns the possibility of exploring the regional differences between upper and lower chest wall movement through the use of accelerometers in individuals breathing while seated.

The two patterns recognized also suggest the coherence between the regional movement measured by accelerometers and the physiology of the sound of breathing (Sarkar et al., 2015). Air movement produces vibrations that result in breathing sounds (Chen et al., 2014). While seated, there is a higher sound intensity, making it possible to hear the inferior portion of the thorax, which results from diaphragm movements for inspiration (Sarkar et al., 2015). These patterns found coherence between the upper zone of the thorax (costal-superior) and the lower zone of the thorax (costal-abdominal) (Ratnovosky et al., 2008; Takashima et al., 2017).

PCA with dimension reduction indicated that the transformation of the segmented magnitude of acceleration to the PCA domain by linear decorrelation of data helped to recognize patterns through a clustering technique, in contrast to the simplest normalizations of datasets with and without applications of k-means, and PCA without dimension reduction (Fig. 3). This procedure is in accordance with data from Prabhu and Anbazhagan (2011), who found better accuracy using PCA and K-means, with K-means performing the worst when high dimensional data existed, due to the presence of outliers. Nevertheless, the PCA with dimension reduction did not show the best physiological distribution of sensors, due to the right and left rib movements being incorporate in different clusters. This limitation may require more advanced data analysis algorithms in future studies, i.e., analysis with non-linear dimension reduction or other clustering.

We consider that the accelerometers localized on the thorax and abdominal wall give important information for obtaining two clusters of movements of the chest-abdominal wall. Furthermore, the pattern found in this research suggests it is possible to measure the regional differences in breathing patterns in a seated posture using accelerometers. Our findings may have clinical applications in rehabilitation programs after acute cardiorespiratory problems by permitting assessment in a seated position through biofeedback, telemedicine control of respiratory exercises, and for chronic patients. However, the feasibility for use in different populations, i.e., thorax abnormalities, children, and others, needs to be further investigated. Future effort are needed to establish the lowest number of sensors necessary to identify both patterns, which also may suffer from the influence of pathological conditions and remains to be compared with other instruments like plethysmography. Another limitation was the relative quality of the signal acquired, which required smoothing.

5. Conclusions

Accelerometers placed on the chest and abdominal wall permit the collection of two clusters of movement regarding respiration biomechanics. Using a machine learning algorithm, we identified two respiration patterns during seated posture, with one cluster related to the superior-costal pattern and the other related to the abdominal pattern.

Funding

This work was supported by CONICYT-Chile Grant No. BASAL FB0008. FCP is supported by a CNPq-Brazil research fellowship.

Declaration of Competing Interest

The authors declare no conflicts of interest.

Acknowledgements

Authors acknowledge the support of FC during data acquisition.

References

Aliverti, A., Quaranta, M., Chakrabarti, B., Albuquerque, A.L., Calverley, P.M., 2009. Paradoxical movement of the lower ribcage at rest and during exercise in COPD patients. Eur. Respir. J. 33 (1), 49–60.
Bianchi, R., Gigliotti, F., Romagnoli, I., Lanini, B., Castellani, C., Binazzi, B., et al., 2007. Patterns of chest wall kinematics during volitional pursed-lip breathing in COPD at rest. Respir. Med. 101 (7), 1412–1418.
Chen, G., de la Cruz, I., Rodriguez-Villegas, E., 2014. Automatic lung tidal volumes estimation from tracheal sounds. Conf. Proc. IEEE Eng. Med. Biol. Soc. 1497–1500.
Drummond, G.B., Bates, A., Mann, J., Arvind, D.K., 2013. Characterization of breathing patterns during patient-controlled opioid analgesia. Br. J. Anaesth. 111 (6), 971–978.
Fekr, A.R., Janidarmian, M., Radecka, K., Zilic, Z., 2016. Respiration disorders classification with informative features for m-health applications. IEEE J. Biomed. Health Inform. 20 (3), 733–747.
Fukakusa, M., Sato, T., Furuhata, H., 1998. Use of an accelerometer to measure coughing. Nihon Kokyuki Gakkai Zasshi 36 (4), 343–346.
Gutiérrez, M.C., Beroíza, T., Borzone, G., Caviedes, I., Céspedes, J., Gutiérrez, M., et al., 2007. Manual of procedures on spirometry. Chilean Society of Respiratory Diseases, 2006. Rev. Chil. Enf. Respir. 23, 31–42.
de Groote, A., Wantier, M., Cheron, G., Estenne, M., Paiva, M., 1997. Chest wall motion during tidal breathing. J. Appl. Physiol. 83 (5), 1531–1537.
Kavanagh, J.J., Menz, H.B., 2008. Accelerometry: a technique for quantifying movement patterns during walking. Gait. Posture 28 (1), 1–15.
Knudson, R.J., Lebowitz, M.D., Holberg, C.J., Burrows, B., 1983. Changes in the normal maximal expiratory flow-volume curve with growth and aging. Am. Rev. Respir. Dis. 127 (6), 72–734.
Liu, H., Guo, S., Zheng, K., Guo, X., Kuramoto-Ahuja, T., Sato, T., et al., 2017. Reliability and validity of measuring respiration movement using a wearable strain sensor in healthy subjects. J. Phys. Ther. Sci. 29 (9), 1543–1547.
Maarsingh, E.J., van Eykern, L.A., Sprikkelman, A.B., Hoekstra, M.O., van Aalderen, W. M., 2000. Respiratory muscle activity measured with a EMG technique: technical aspects and reproducibility. J Appl Physiol (1985);88(6):1955–61.
Massaroni, C., Senesi, G., Schena, E., Silvestri, S., 2017. Analysis of breathing via optoelectronic systems: comparison of four methods for computing breathing volumes and thoraco-abdominal motion pattern. Comput. Methods Biomech. Biomed. Eng. 20 (16), 1678–1689.
Mesquita Montes, A., Maia, J., Crasto, C., de Melo, C.A., Carvalho, P., Santos, R., et al., 2017. Abdominal muscle activity during breathing in different postures in COPD "Stage 0" and healthy subjects. Respir. Physiol. Neurobiol. 238, 14–22.
Miller, M.R., Hankinson, J., Brusasco, V., et al., 2005. Standardization of spirometry. Eur. Respir. J. 26 (2), 319–338.
Prabhu, Anbazhagan, 2011. Improving the performance of k-means clustering for high dimensional data set. Int. J. Comput. Sci. Eng. 3 (6), 2317–2322.
Price, K., Schartz, P., Watson, A., 2014. The effect of standing and sitting postures on breathing in brass players. Springerplus 3, 210.
Ratnovsky, A., Elad, D., Halpern, P., 2008. Mechanics of respiratory muscles. Respir. Physiol. Neurobiol. 163 (1–3), 82–89.
Reifferscheid, F., Elke, G., Pulletz, S., Gawelczyk, B., Lautenschläger, I., Steinfath, M., et al., 2011. Regional ventilation distribution determined by electrical impedance tomography: reproducibility and effects of posture and chest plane. Respirology 16 (3), 523–531.
Robergs, R., Dwyer, D., Astorino, T., 2010. Recommendations for improved data processing from expired gas analysis indirect calorimetry. Sports Med. 40 (2), 95–111.
Sarkar, M., Madabhavi, I., Niranjan, N., Dogra, M., 2015. Auscultation of the respiratory system. Ann. Thorac. Med. 10 (3), 158–168.
Stendardi, L., Binazzi, B., Scano, G., 2007. Exercise dyspnea in patients with COPD. Int. J. Chron. Obstruct. Pulmon. Dis. 2 (4), 429–439.
Ragnarsdóttir, M., Kristinsdóttir, E.K., 2006. Breathing movements and breathing patterns among healthy men and women 20–69 years of age. Reference values. Respiration 73 (1), 48–54.
Takashima, S., Nozoe, M., Mase, K., Kouyama, Y., Matsushita, K., Ando, H., 2017. Effects of posture on chest-wall configuration and motion during tidal breathing in normal men. J. Phys. Ther. Sci. 29 (1), 29–34.
Takazakura, R., Takahashi, M., Nitta, N., Murata, K., 2004. Diaphragmatic motion in the sitting and supine positions: healthy subject study using a vertically open magnetic resonance system. J. Magn. Reson. Imaging 19 (5), 605–609.
Ziegler, B., Fernandes, A.K., Sanches, P.R., Konzen, G.L., Dalcin, P.T.R., 2015. Variability of the perception of dyspnea in healthy subjects assessed through inspiratory resistive loading. J. Bras. Pneumol. 41 (2), 143–150.

Carlos De la Fuente received the B.S. degree in physical therapy at the Universidad Mayor (2011), is candidate of Msc. in Engineering Sciences at Universidad de Valparaiso (Chile) and candidate of Msc. in Kinesiology and Clinical Biomechanics at Universidad Metropolitana de Ciencias de la Eduación. In 2015 received the young investigator award by International Society of Biomechanics and Brazilian Society of Biomechanics in Florianopolis. Currently, is student member of ISB and BSB and his research interests include clinical biomechanics, cadaveric biomechanics, digital signal processing, and computational intelligence applied to human movement science.

Alejandro Weinstein is a professor at the School of Biomedical Engineering of the Universidad de Valparaiso, Chile. He received the B.S. degree in electronics engineering from the Universidad Técnica Federico Santa María (2000). He received the Ph.D. in electrical engineering, with an emphasis in signal processing, from the Colorado School of Mines (2013). His current research interests include bioinstrumentation, biomedical signal processing, and neuromodulation techniques.

Rodrigo Guzmán-Venegas graduated in Kinesiology from Católica del Maule University, Chile, and obtained his MSc. in Biophysics from the University of Chile. He is teaching Biophysics and Biomechanics at los Andes University, Chile. He is currently taking part in the Integrative Laboratory of Biomechanics and Effort Physiology (LIBFE) in los Andes University. His research interests are in the areas of processing of biomedical signals, human motion analysis and applied physiology of the neuromuscular system.

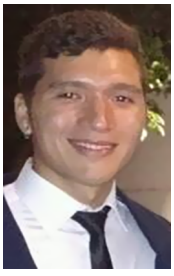

Juan Arenas Muñoz is graduated in physiotherapy at the Pontificia Universidad Católica de Chile.

His research interests include gerontological physioterapy.

Jorge Cartes Ibáñez is graduated in physiotherapy at the Pontificia Universidad Católica de Chile.

He is student of Manual Therapy and Pain. His research interests include biomechanics applied to the clinical musculoskeletal physiotherapy.

Marco Antonio Soto is graduated in physiotherapy at the Pontificia Universidad Católica de Chile. He is student of Respiratory Care for Physiotherapists at the Universidad de Chile. His research interests include Clinical Respiratory Physiotherapy.

Felipe P Carpes, Brazil. Carpes is a professor at the Center for Health Sciences of the Federal University of Pampa, in Brazil. He is the current president of the Brazilian Society of Biomechanics and member of the Executive Council of the International Society of Biomechanics. His research focuses on developing a basic understanding of the production and regulation of movements with studies in humans and other animal models, and applying this information to training and rehabilitation. Carpes also dedicates to help different groups across the world to establish laboratory and research groups in the field of biomechanics, and the organization of new biomechanics societies in EDC.